


A micro-CT investigation of densification in pressboard due to compression

R. Afshar¹  | J. Stjärnesund¹ | E. K. Gamstedt¹ | O. Girlanda² |
F. Sahlén³ | D. Tjahjanto⁴

¹Department of Materials Science and Engineering, Division of Applied Mechanics, Uppsala University, Uppsala, Sweden

²Hitachi Energy Research Sweden, Västerås, Sweden

³ABB Corporate Research, Västerås, Sweden

⁴NKT HV Cables AB - Technology Consulting, Västerås, Sweden

Correspondence

R. Afshar, Department of Materials Science and Engineering, Uppsala University, Box 35, SE-751 03 Uppsala, Sweden.

Email: reza.afshar@angstrom.uu.se

Abstract

As a non-destructive inspection method, micro-computed tomography has been employed for determining local properties of a cellulose-based product, specifically pressboard. Furthermore, by utilizing the determined properties in a detailed numerical model, by means of a finite element analysis, we demonstrate a continuum anisotropic viscoelastic-viscoplastic model. Through such a combination of non-invasive experiments with accurate computations in mechanics, we attain a better understanding of materials and its structural integrity at a pre-production stage increasing the success of the first prototype. In detail, this combination of micro-computed tomography and finite element analysis improves accuracy in predicting materials response by taking into account the local material variations. Specifically, we have performed indentation tests and scanned the internal structure of the specimen for analysing the densification patterns within the material. Subsequently, we have used a developed material model for predicting the response of material to indentation. We have computed the indentation test itself by simulating the mechanical response of high-density cellulose-based materials. In the end, we have observed that pressboard, having initially a heterogeneous density distribution through the thickness, shows a shift in the densification to the more porous part after indentation. The densification maps of the simulated results are presented by comparing with the experimental results. A reasonable agreement is observed between the experimental and the simulated densifications patterns, which suggests that the proposed methodology can be used to predict densification also for other fibre-based materials during manufacturing or in service loading.

KEYWORDS

densification, finite element method, indentation test, micro-computed tomography, pressboard

This is an open access article under the terms of the [Creative Commons Attribution-NonCommercial](https://creativecommons.org/licenses/by-nc/4.0/) License, which permits use, distribution and reproduction in any medium, provided the original work is properly cited and is not used for commercial purposes.

© 2023 The Authors. *Strain* published by John Wiley & Sons Ltd.

1 | INTRODUCTION

Understanding the behaviour of heterogeneous materials such as cellulose materials (paper, wood and wood products) in micro/nano scale is essential in understanding of their mechanics. Cellulose materials are composed of various intricate microstructures at different length scales: from the molecular structure of the microfibrils, the arrangement of microfibrils in a lignin/hemicellulose matrix constituting the fibre substructures, up to the network of cellulose fibres on a macroscopic level. Therefore, such cellulose-based materials exhibit complex deformation mechanisms with intricate anisotropic behaviour at various length scales. The anisotropy at the level of single fibre can be related to the orientation of the fibril-lignin composite structure (twist) within the cell-wall layers and the arrangement of the layers composing the fibre wall.^[1,2] At the higher scale, the level of (macroscale) fibre-pore network, anisotropic behaviour is mainly due to the spatial arrangement of the fibres in the network.^[3]

The strength of paper depends mainly on the strength of the individual fibres and the strength of the fibre to fibre joints.^[4,5] In Jajcinovic et al,^[5] the first direct measurements of breaking loads of individual eucalyptus fibres and fibre to fibre joints are presented. In another study,^[6] by using atomic force microscopy, the mechanical properties of individual fibre-to-fibre bonds on the nanometre scale in terms of the total energy input and time dependent processes are studied. They showed that fibrils or fibril bundles play a crucial role in fibre-fibre bonding because they act as bridging elements. Due to the high density of the fibre networks, cellulose-based materials are often seen as a solid material product at the macroscopic scale.

Pressboard is a high-density cellulose-based composite material with the presence of fibres. It is a structurally complex multiscale material. Also, it is a porous material, which is typical for wood-based materials. The bulk of pressboard is composed of a network built by high-strength slender natural fibres. These fibres are bonded or entangled to each other. The spatial distribution of the fibres causes the in-plane direction to be intrinsically stronger and stiffer than the out of-plane one. The aforementioned compressive forces act along the thickness, that is, weakest direction of the material. Pressboard also presents the characteristic behaviour of a porous material, as irregular-shaped voids appear in the fibre network. The pores combined with the high flexibility of the fibres manage pressboard to withstand large stress and large deformation without causing failure. The large permanent deformations are caused by a reduction of the pore size and a compression of the fibres. Therefore, this macroscale behaviour is caused by the presence of the microscale structure. Such a multiscale materials description is fairly challenging to discern the contribution of different length-scales. Pressboard is used in fluid-filled power transformers both as dielectric material and as load-bearing element. During operation, pressboard is loaded by several mechanical cyclic forces in form of vibrations.^[7] One particularly harsh loading condition during operation is short circuiting of the transformer, as some components are subjected to high compressive forces in very high rates. As a result of these forces, plastic deformations are likely to be generated.

A material model to describe the compressive behaviour of pressboard is presented in Tjahjanto et al.^[3] However, a study of the microscopic mechanical behaviour with attention to internal changes in the material is needed. This paper investigates the mechanisms responsible for permanent deformations in pressboard subjected to high compressive loads. The workflow of the study is shown in Figure 1 and describes how experiments and simulations results are employed for evaluation and comparison.

In particular, the experiments and simulations focus on the changes in density distribution through the thickness of the material, when load is applied along the out-of-plane direction (through-thickness). With a micro-computed tomography (μ CT), the interior of pressboard is studied before and after deformation. This approach has been used in the literature^[3,8] for other types of materials. Furthermore, a finite element model has been created comparing simulations with the experimental ones. As already used in previous studies,^[9,10] the combination of μ CT and the finite element analysis (FEA) is propitious for obtaining better predictions in engineering design.

2 | MATERIAL AND METHODS

We have performed through-thickness compression tests on pressboards. In particular, the structure was subjected to an indentation on the surface, with a spherical indenter out of steel. This configuration is chosen for the following reasons. First, the concentrated compressive load is between the surface of the sphere and the top surface of the pressboard. This positioning has been chosen since, in the configuration of a transformer winding, the conductors press on the surface of pressboard spacers. Second, there is a limitation in the size of the CT scan's observable area. Hence, the

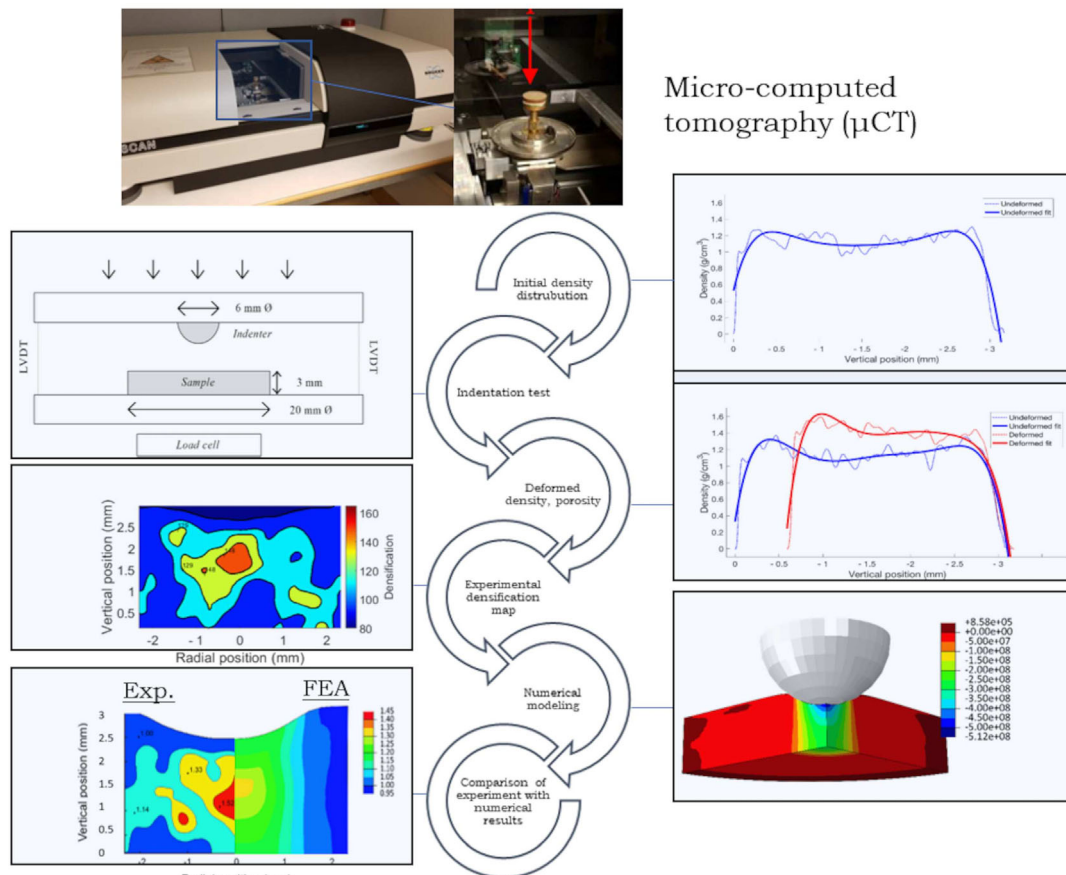


FIGURE 1 Workflow of the study.

pressboard specimen is chosen to be of a circular shape. This arrangement allowed for the accurate measurement of deformations and mass density changes within the material focusing on the area below the indentation sphere.

Before the tests, the pressboard samples were scanned using μ CT method to define their initial (mass) density distribution profiles along the thickness direction. The samples were then subjected to different levels of compressive forces applied by the indenter. During the experiments, the load–displacement curve of each test piece was recorded.

After indentation test, upon removal of the load, the densification map was reconstructed for the area of permanent plastic deformation underneath the indenter. This map was then analysed in a μ CT Analyser software. The density distribution before and after the indentation was used for validation of a numerical simulation by means of the finite element method.

2.1 | Material

The material is known as pressboard, a high-density paper material used in electrical transformers as an insulator. Pressboard is produced with unbleached kraft pulp of electrical grade. During the production stage, the sheets of unbleached kraft pulp of electrical grade are pressed between heated plates with meshes to produce high density pressboard. The meshes create permanent wavy pattern on the surface material, so-called wire marks, which affect the density distribution well within the material.^[11] In order to reduce the surface unevenness, the surface of the material is polished, giving a product known as calibrated material.

In this paper, 3 mm thick calibrated high-density pressboard was used, with a density between 1.1 and 1.2 g/cm³. We emphasize that the density of the polymers making up paper is 1.5 g/cm³, while pressboard is built by a porous network of fibres. Figure 2 shows the final product, pressboard and its porous microstructure taken by SEM (scanning electron microscopy).

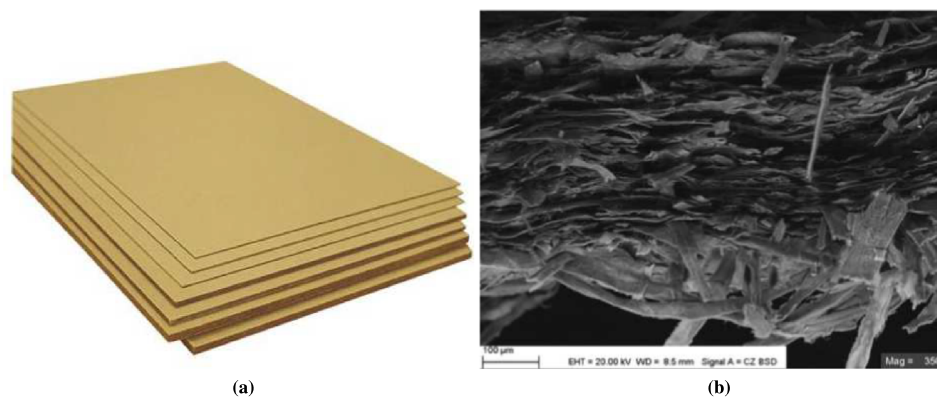


FIGURE 2 (a) Pressboard in different thicknesses (Hitachi Energy Figeholm). (b) Cross section in the thickness direction (K. Wei and F. Sahlén)

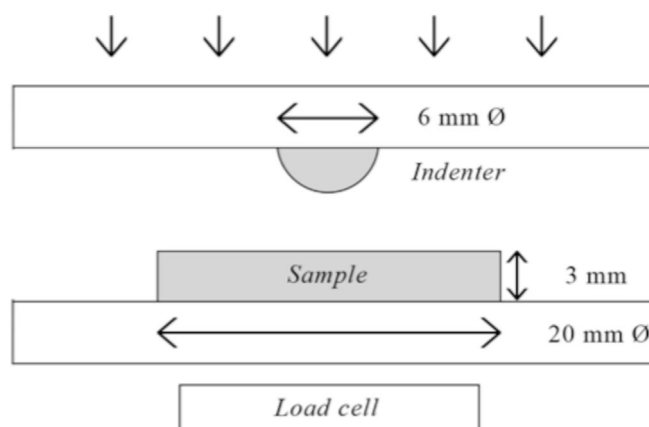


FIGURE 3 Sketch of the setup used for mechanical loading of the samples.

2.2 | Sample preparation and mechanical loading

Pressboard specimens were produced by cutting 3 mm thick plates into cylindrical samples with a diameter of 20 mm. This geometry is allowing an improved image quality in CT-scans, as described in Bruker.^[12] The samples were then subjected to a concentrated load by indentation with a 6 mm diameter spherical steel ball, in order to induce localized high loads. Test setup is shown in detail in Figure 3. Each sample was loaded with a single indentation where the maximum force was 700 N, 1400 N, or 2800 N. These forces correspond to the mean contact pressure of 90, 120 and 150 MPa, according to the Hertzian contact stress.^[13] The purpose of the three load cases was to create remaining deformations with calculated stresses in the 90–150 MPa interval, similar to the allowed stress range on pressboard spacers during short circuit.^[14] The spherical indenter was chosen for a simplified test setup. Displacement was measured by three displacement transducers.

2.3 | Micro-CT scanning and reconstruction

The μ CT uses X-rays for imaging. This method enables non-invasive investigation and visualizing of the interior of the material. The μ CT scans in this investigation were carried out by using a Bruker Skyscan 1172 desktop style. All the samples were scanned both before and after mechanical loading. The voxel sizes of the images are in the micrometre range, and due to the cone-shaped X-ray beam, the voxel sizes were determined by the distance between the X-ray source and sample. The resulting voxel size in this investigation was 10.6 μ m. The voxel size was chosen based on the size of the sample and the output parameter. Since, in this study, our aim was to measure density and density

distribution, thus, a high level of details was not required and larger voxel size could then be selected to reduce the scanning time. During the scans, the X-ray source voltage was set to 80 kV, current to 125 μA and exposure time to 850 ms. These parameters were tested for the intensities to fall within recommended limits.^[15] A thin aluminium filter (thickness of 0.5 mm) was placed in front of the X-ray source to reduce so-called beam hardening artefacts. The projections were recorded with a rotation increment of 0.4° within 180° . The scanning time was ~ 1 h.

The reconstructions were made in the software NRecon V.1.7.0.4. Smoothing was done with Gaussian kernel level 10 to reduce noise and get a clearer picture of the density distribution. Ring artefacts were removed by Ring Artefact Correction level 20. Despite the aluminium filter in the μCT , some beam hardening artefact still appeared. This artefact was extracted with 35 % Beam Hardening Correction.

2.4 | Image analysis

The reconstructed images were analysed in CT Analyser V.1.16.4.1, Fiji and Matlab. With the average grey value from the μCT and the measured density of a specimen, the greyscale is translated into density by assuming a linear relationship between them. The results from the image analysis are shown as either line profiles or contour maps. The profiles of the density versus distance are obtained in Fiji, according to a reference line from the top surface to the bottom of the sample as demonstrated in Figure 4.

Contour maps of the cross sections are created in Matlab. The images are first smoothed with ImGaussfilt level 16 for making a more homogeneous greyscale distribution. The smoothing disturbs the transition from specimen to air. As an edge-preserving action, voxels in the images below the grey value of 50 have been replaced by 0. The level of contour was set to 8. In order to visualize where in the samples the change of density has occurred, densification maps were created. The densification is defined according to Equation (1):

$$D(\chi) = \frac{\rho'(\chi)}{\rho(\chi)} \quad (1)$$

where $D(\chi)$ is the densification ratio, $\rho(\chi)$ is the density of voxel χ in the undeformed state and $\rho'(\chi)$ is the density of voxel χ in the deformed state.

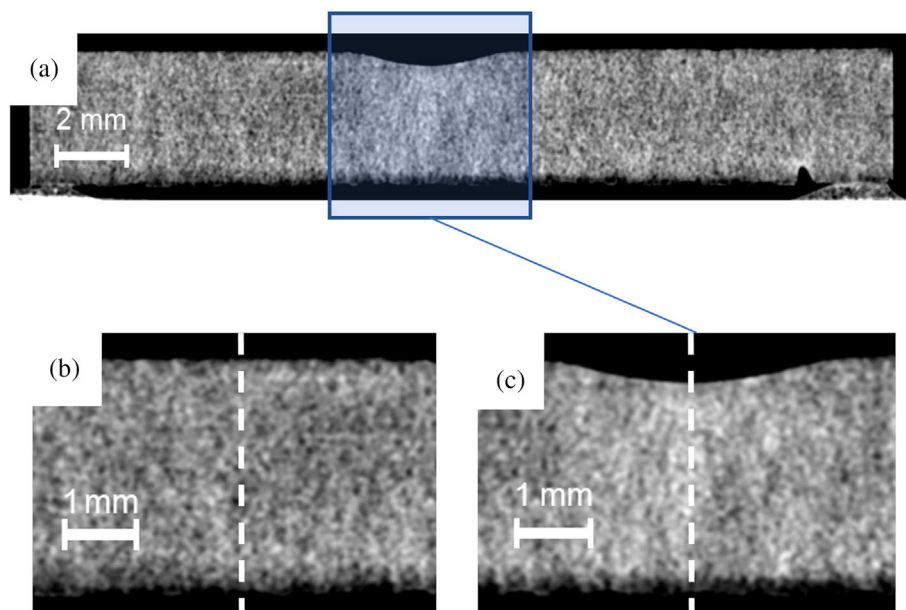


FIGURE 4 Scanned cross-section of a sample with final/left-over deformation (a) and the line in which the density versus distance was measured through the thickness, before (b) and after (c) loading.

2.5 | Simulation by the finite element method

Measured as densification, the inelastic deformation is possible to compute by means of a finite element analysis (FEA). A continuum material model is developed in Tjahjanto et al.^[3] for describing the mechanical responses of high-density cellulose-based fibre materials subjected to various loads at standard room conditions. The model is utilizing infinitesimal strains assumption such that the total strain is decomposed additively into elastic and plastic parts. The main features of the model include (i) anisotropic material properties, (ii) viscoelasticity, (iii) rate-dependent viscoplastic behaviour, (iv) anisotropic hardening with a kinematic effect and (v) material densification due to through-thickness compression. The model is called anisotropic viscoelastic-viscoplastic (VE-VP) model, and its detailed formulations have been reported in Tjahjanto et al.^[3] There is also a simplified 1-D formulation of this model, considering only the out-of-plane normal direction, reported in Girlanda et al.^[16]

All material parameters for anisotropic VE-VP continuum model were exactly the same as those used in Tjahjanto et al.^[3] because, first, they were the same pressboard material and, second, the tests were performed under the same climate conditions (standard room condition 23°C, 50%RH, i.e., relative humidity). In fact, although the calibration of the material parameters shown in Tjahjanto et al.^[3] was made under simple load/boundary conditions, for example, uniaxial tension/compression, but the calibration procedure has been properly done, such that the same material parameters can still capture the behaviour of pressboard under a different, more-complex loading (i.e., indentation). The only input parameters that were particularly adjusted for the present work were the initial porosity/density. Based on the micro-CT measurement, the initial porosity/density of the pressboard was varied across the thickness direction, as indicated in Figure 6. This inhomogeneous initial porosity has been taken into account in the model simulation.

We stress an important assumption in the simulations that the maximum material density of pressboard has been set to 1.5 g/cm³, based on the theoretical value for cellulose. This theoretical limit is the upper threshold so that the densification during compression will not go beyond 1.5 g/cm³, the density of the cellulose. In another words, we assume that by reaching 1.5 g/cm³, we have compressed out all pores within the fibre network, in other words, zero porosity. An FE model for 20 mm diameter pressboard of 3 mm thick with 6 mm diameter spherical steel indenter before and after indentation is shown in Figure 5 on the left and right sides, respectively.

3 | RESULTS AND DISCUSSION

3.1 | Density distribution

The CT results are presented in Figure 6 as (mass) density variation with respect to vertical position of undeformed pressboard, before loading. The x-axis goes from 0 to −3 mm, where 0 denotes the top surface and −3 mm is the bottom. The dashed line is obtained from scanning results, and the solid one is its corresponding fit-curve by a polynomial function of order 6. Obviously, there is an inhomogeneous density distribution through the thickness, with a reduction of density at both surfaces and in the middle of the specimen. There are two possible explanations for the lower density at the surfaces: The first is the coarse surface due to the wire marks from the fabrication, and the other is that the images are smoothed leading to loss of sharpness in edges. This type of density distribution has been seen in thinner machine-made paper products before.^[17]

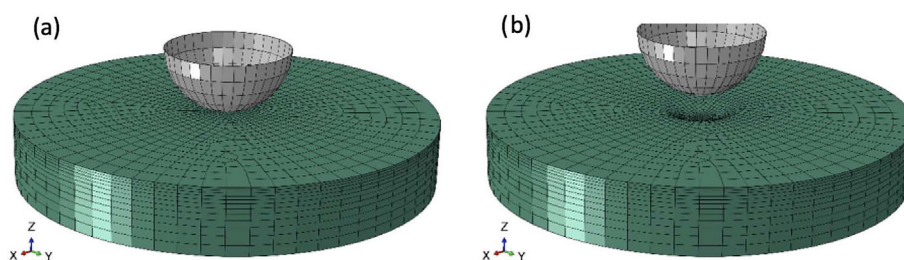


FIGURE 5 Finite element (FE) model for 20 mm diameter pressboard of 3 mm thick with 6 mm diameter spherical steel indenter, (a) before and (b) after indentation.

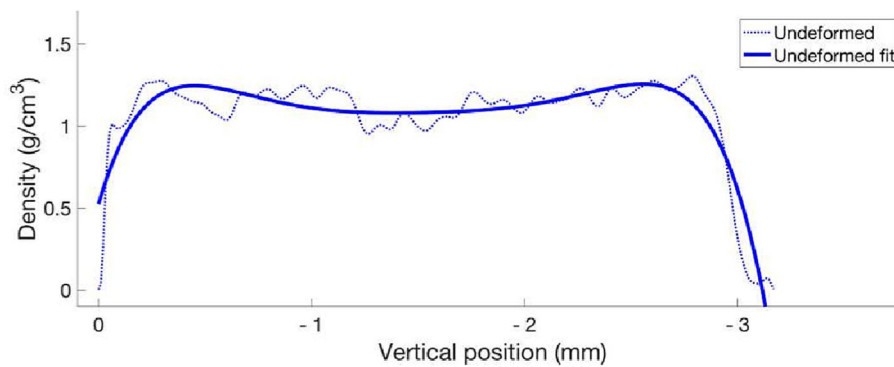


FIGURE 6 Density versus distance for an undeformed sample.

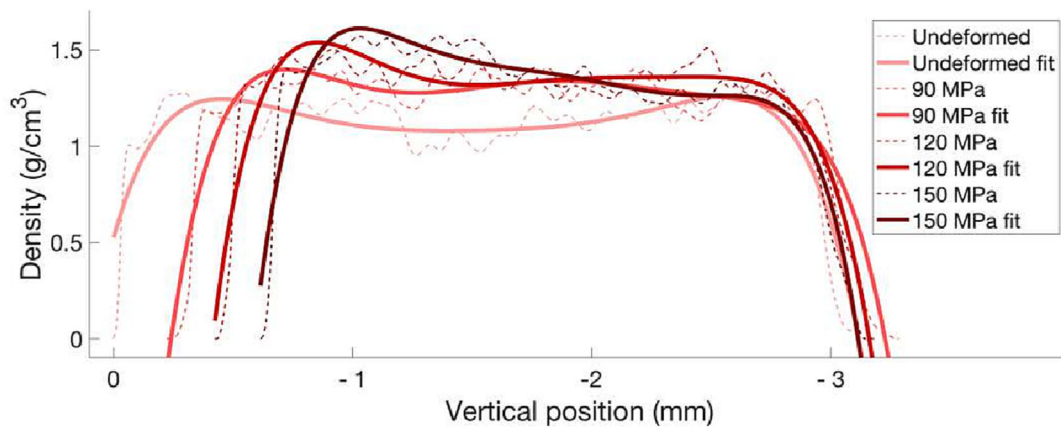


FIGURE 7 Comparison of density versus distance for undeformed and deformed samples. The measurement position is defined in Figure 4

Figure 7 demonstrates all results, dashed lines from measurement data and continuous lines as their corresponding fit-curves. For different loading cases of 90, 120 and 150 MPa, a comparison is visible before and after deformation. The measurement position in Figure 7 is defined in Figure 4. The profiles are displayed with different intensity of the red colour. The curves become darker with increasing applied loading, thus deformation. For the case of 90 MPa load, it is observed that the density is more homogeneous than unreformed case. Besides the densified area in the middle, the 120 MPa case shows an increased density from the indentation side. Analogously in the 150 MPa case, we observe an even more increased density to the indentation side.

These density profiles indicate that two mechanisms occur simultaneously within the material under loading. The first mechanism is that the more porous part in the middle of the thickness of the sample appears to densify first. This behaviour could be explained by the fact that structure is mechanically weaker where the material is more porous. Hence, these sections are more prone to deformation. The second mechanism is when the density has become more homogeneous throughout the specimen, further deformation has led to densification at the indentation side. The density is obviously highest on the deformation side after unloading. Figure 8 shows the densification process for different loading cases schematically.

3.2 | Force-indentation depth, density, densification factor and porosity distribution

For a direct comparison between the FEM results and experiments, we present force–displacement curves, mass density, porosity and densification factor along the thickness of the samples in the case of 90, 120 and 150 MPa cases in Figures 9–11. The FEM results are using the VE-VP model; before indentation, the densification is one, and initial mass density and porosity are taken from the measurements. During the indentation test, the force is increased and max load is hold for a time to release the creep deformation and then unloading is performed. Repeatability in experiments is a

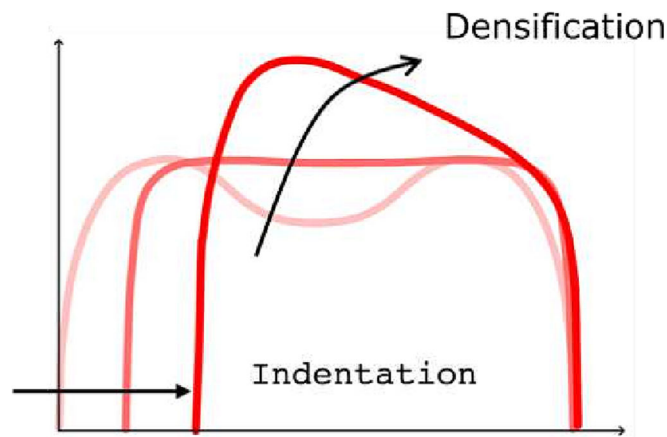


FIGURE 8 Schematic illustration of how the density is changed by deformation.

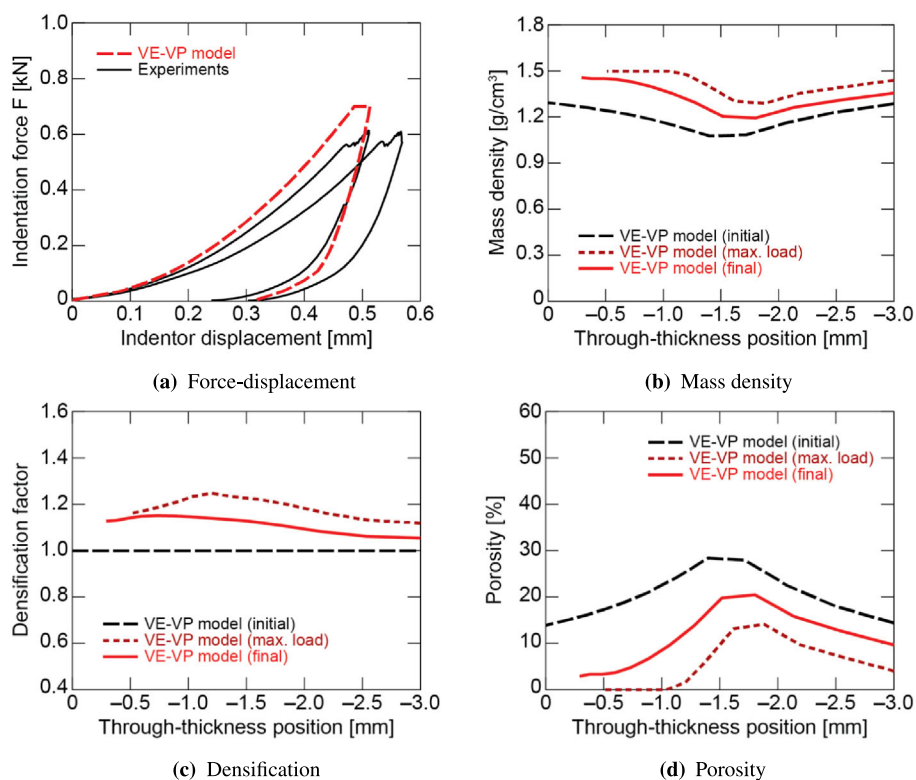


FIGURE 9 (a) Force-indentation depth, (b) density, (c) densification factor and (d) porosity distribution for maximum indentation force 700 N (corresponding to mean contact pressure 90 MPa)

challenge in indentation test since the material is heterogeneous with a microstructure directly affecting the indenter response.

As it is obvious from Figure 9, the comparison of computation with experiments in force-indentation curves, under 90 MPa loading, shows a good agreement, considering the scattered experimental data. The plastic deformation is underestimated in the computational model.

The mass density along the thickness of the sample using the VE-VP model is the lowest at the middle of the sample (for initial, maximum load and final/after release of indenter). Accordingly, the porosity becomes the highest at the middle of the sample, although the maximum location varies for initial, maximum load and final/after release of indenter. The densification factor has a highest value near the top surface under the indenter. Yet again, its maximum location varies for maximum load and final/after release of indenter (initially the densification factor is constant).

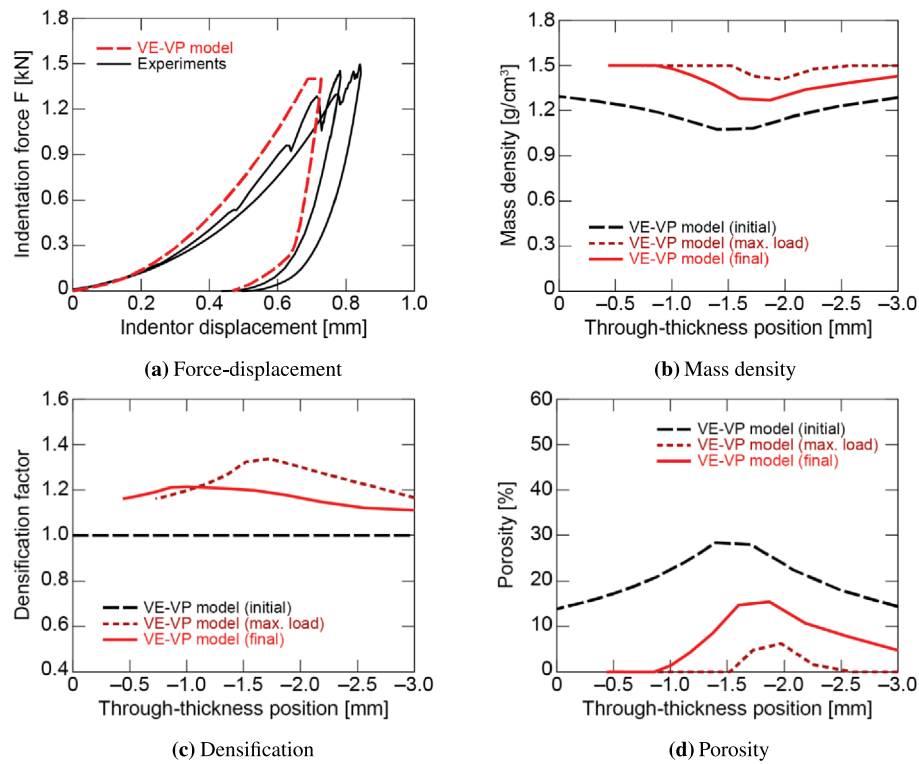


FIGURE 10 (a) Force-indentation depth, (b) density, (c) densification factor and (d) porosity distribution for maximum indentation force 1400 N (corresponding to mean contact pressure 120 MPa)

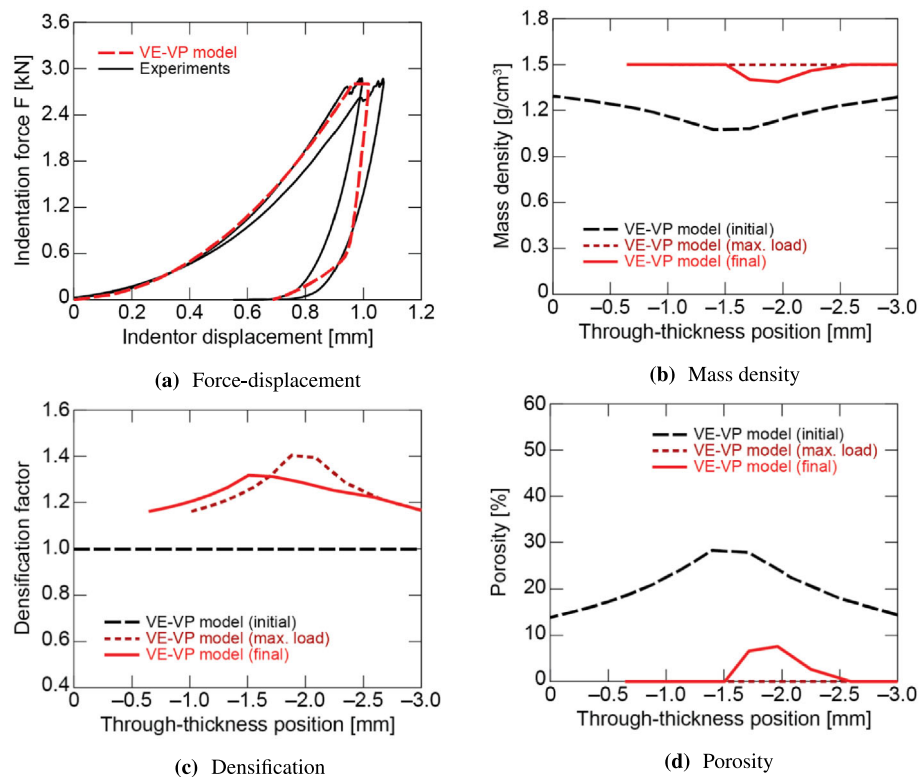


FIGURE 11 (a) Force-indentation depth, (b) density, (c) densification factor and (d) porosity distribution for maximum indentation force 2800 N (corresponding to mean contact pressure 150 MPa)

From Figure 10, the numerical force-indentation depth curves, under 120 MPa loading, have some deviation from experiments. However, the plastic deformations (measured as the permanent/left-over indentation depth) are close in both cases.

The trends for mass density, porosity and densification factor are similar to those from Figure 9.

Analogously in Figure 11, we see a convincing agreement. We stress that the FEM model is using the same set of parameters in all cases. The trends for mass density, porosity and densification factor are also analogous to Figure 9.

Considering only the final/after release of indenter deformations, a comparison of densification factor and porosity of the samples for different level of maximum indentation force is given in Figure 12.

Furthermore, the comparison of experimental permanent/left-over indentation depth (final/after release of indenter) with the corresponding simulation results for each loading case is summarized in Table 1.

As Table 1 indicates, the agreement between experiment and simulations improves as the indentation force increases. Roughly speaking, the accuracy is 30% more in the higher loading case than the lower loading. This deviation is due to the fact that the higher loading is causing more viscoplastic deformation. This tendency is partly visible in load-displacement curves as well. Hence, we conclude that the viscoplasticity behaviour is captured more accurately in the VE-VP model. In other words, the model parameters for the short range lack the same accuracy as the viscoplastic (long-range) parameters. The calibration of all parameters was mainly done under (1) quasi-static loading and (2) long-range transient like creep and relaxation.^[3]

3.3 | Densification maps

We present some of the experimental work; for more details, we refer to Stjarnesund.^[18] One important aspect is that the comparison is performed in a qualitative manner between numerical results and experiments. We circumvent ourselves from expecting more from the continuum VE-VP model than it has been developed for, namely, for larger length scale. The resolution of the present FEA model is 0.1 mm, which is about the size of several fibres.

In order to compare the densification results from computation and experiments, we present the results side-by-side. Contour maps of the densification in the specimens' cross sections are shown in Figure 13. On the left, experimental densification results are places, whereas on the right side, we show the computational results in different colour scales.

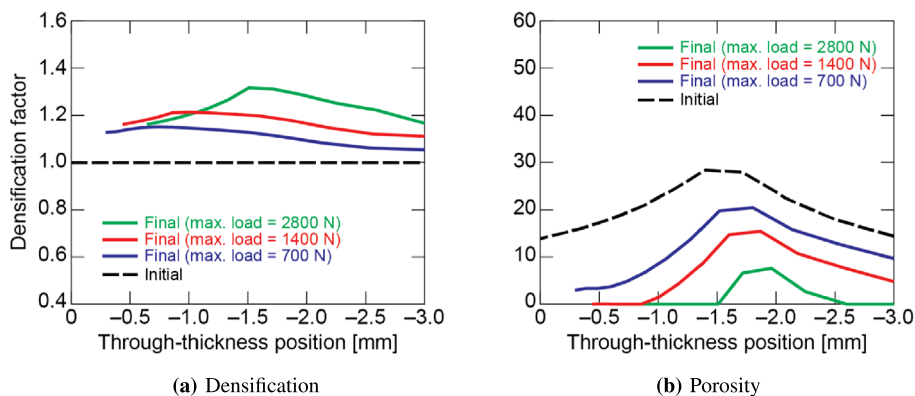


FIGURE 12 (a) Densification factor and (b) porosity of pressboard after indentation (final) for different level of maximum indentation force.

TABLE 1 Comparison of experimental permanent/left-over indentation depth with the corresponding simulation results for each loading case.

Loading case (MPa)	Experiment (mm)	Simulation (mm)
90 (700 N)	0.25	0.32
120 (1400 N)	0.45	0.44
150 (2800 N)	0.65	0.65

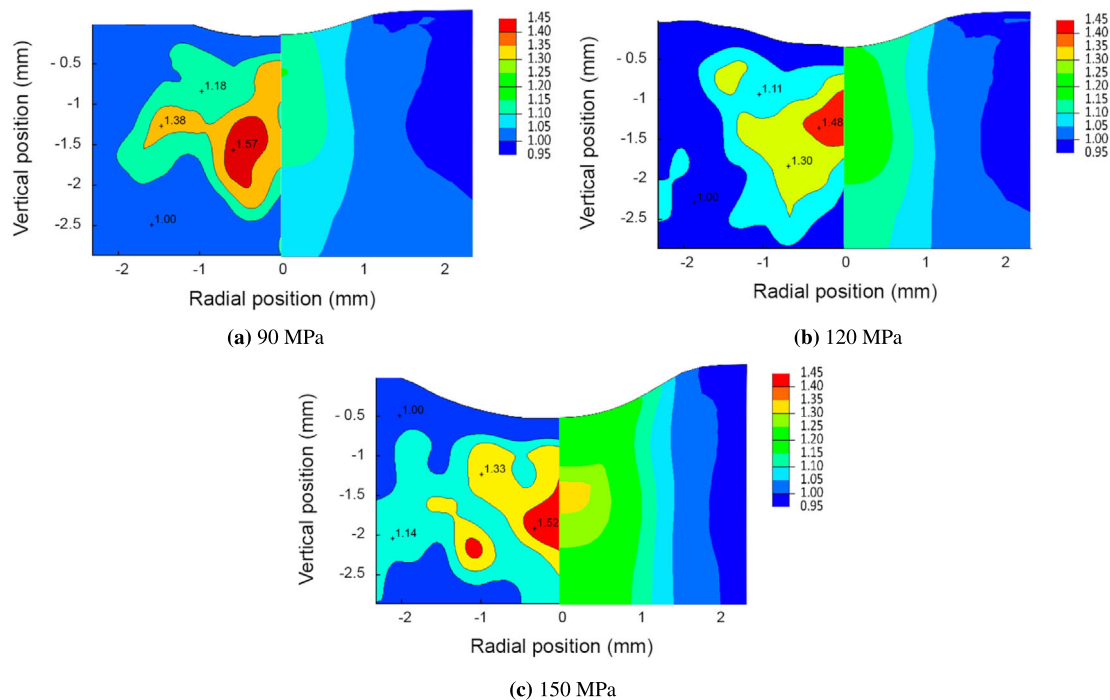


FIGURE 13 Density map of different load cases: experimental result to the left and FEA result to the right: (a) 90 MPa; (b) 120 MPa; (c) 150 MPa.

The results are on the cut profile, such that the axes denote vertical and radial positions. The applied force is placed at the position (0, 0), that is, the top surface.

Experimentally, in all load cases, the maximum densification tends to occur in the middle of the thickness. However, numerically, this behaviour becomes more evident as the load increases (Figure 13a). This observation is easily justified since we know from density profiles that the specimens are mechanically weaker in the middle due to a higher porosity, hence a lower stiffness. In the both experimental and numerical results, the maximum densifications for all loading case reach to around 1.50, which is the theoretical value for cellulose. This could be explained by the fact that the densification of the material is saturated at a certain level when the porosity is very small or absent. We stress that, experimentally, the initial density $\rho(\chi)$ is varying along the thickness of the specimen, as shown in Figure 7, whereas, numerically, it is set to $\rho(\chi) = 1$, as can be seen in Figure 12.

In addition, the distribution of densification maps is more uniform in numerical results, which is expected due to the homogeneity assumption of the continuum FE model, indeed by contrast to the case in reality.

4 | CONCLUSIONS

The μ CT method is well suited to investigate the internal structures and density changes in pressboard. This fibre-based material is similar in structure to paper and packaging board, and the methodology can be applied to other compressible fibre materials. The μ CT provides a non-destructive analysis of local density variations within such materials. The density through samples before loading has demonstrated that the initial material is heterogeneous, with a reduction of density at both surfaces and in the middle of the specimen. By introducing a measure for quantifying the mass density change with respect to the initial value, we have performed experiments for obtaining the so-called densification. The maximum densifications in the experiments have been all around 1.50, regardless of the loading cases. The FE simulations describing the indentation test included a continuum anisotropic viscoelastic-viscoplastic model, used for simulating the mechanical response of high-density cellulose-based materials. A reasonable agreement is observed between the experimental and the simulated densifications patterns. The distribution of densification maps is more uniform in numerical results, which is expected due to the homogeneity assumption of the continuum FE model for the sake of simplification. Indeed, material parameters vary in a stochastic manner, and we leave such a study to future research.

ACKNOWLEDGEMENTS

The authors would like to thank B.E. Abali for his help in editing the manuscript and for fruitful discussions. Also thanks to the UU innovation for AIMday financial support, which made the present collaboration possible.

CONFLICT OF INTEREST STATEMENT

The authors declare no potential conflict of interests.

DATA AVAILABILITY STATEMENT

The data that support the findings of this study are available from the corresponding author on reasonable request.

ORCID

R. Afshar  <https://orcid.org/0000-0003-3384-3971>

REFERENCES

- [1] J.-L. Wertz, O. Bédué, O. Bédué, J. P. Mercier, *Cellulose Science and Technology*, EPFL Press **2010**.
- [2] M. Alava, K. Niskanen, *Rep. Prog. Phys.* **2006**, 69(3), 669.
- [3] D. D. Tjahjanto, O. Girlanda, S. Östlund, *J. Mech. Phys. Solids* **2015**, 84, 1.
- [4] A. Torgnysdotter, L. WaBgberg, *Nordic Pulp Paper Res. J.* **2003**, 18(4), 455.
- [5] M. Jajcinovic, W. J. Fischer, U. Hirn, W. Bauer, *Cellulose* **2016**, 23, 2049.
- [6] F. J. Schmied, C. Teichert, L. Kappel, U. Hirn, W. Bauer, R. Schennach, *Sci. Rep.* **2013**, 3(1), 2432.
- [7] G. Bertagnolli, *The ABB Approach to Short-Circuit Duty of Power Transformers* **2007**.
- [8] F. Pierron, S. A. McDonald, D. Hollis, J. Fu, P. J. Withers, A. Alderson, *Strain* **2013**, 49(6), 467.
- [9] Y. Chen, E. Dall, E. Sales, K. Manda, R. Wallace, P. Pankaj, M. Viceconti, *J. Mech. Behav. Biomed. Mater.* **2017**, 65, 644.
- [10] N. Tsafnat, N. Amanat, A. S. Jones, *Fuel* **2011**, 90(1), 384.
- [11] O. Girlanda, F. Sahlén, T. Joffe, E. K. Gamstedt, L. E. Schmidt, F. Forsberg, M. Sjö Dahl, Analysis of the Micromechanical Deformation in Pressboard Performed by X-Ray Microtomography, in 2015 IEEE Electrical Insulation Conference (EIC), IEEE **2015**, 89.
- [12] Bruker, Skyscan 1172 Micro-CT: Scanner Operations, **2008**.
- [13] J. R. Barber, *Contact Mechanics*, Springer **2018**.
- [14] Power Transformers—Part, *IEC Standard*.
- [15] M. F. V. Tarplee, N. Corps, Acquiring Optimal Quality X-Ray μ CT Scans.
- [16] O. Girlanda, D. D. Tjahjanto, S. Östlund, L. E. Schmidt, *J. Mater. Sci.* **2016**, 51(17), 8131.
- [17] R. E. Mark, J. Borch, C. Habeger, *Handbook of Physical Testing of Paper*, 1, Crc Press **2002**.
- [18] J. Stjärnesund, A Micro-CT Investigation of Density Changes in Pressboard due to Compression, **2018**.

How to cite this article: R. Afshar, J. Stjärnesund, E. K. Gamstedt, O. Girlanda, F. Sahlén, D. Tjahjanto, *Strain* **2023**, 59(4), e12442. <https://doi.org/10.1111/str.12442>